Mechanisms Associated with the "Plateau" Observed at High Voltage for the Overlithiated $Li_{1.12}(Ni_{0.425}Mn_{0.425}Co_{0.15})_{0.88}O_2$ System

N. Tran,[†] L. Croguennec,*[,†] M. Ménétrier,[†] F. Weill,[†,‡] Ph. Biensan,[§] C. Jordy,[§] and C. Delmas[†]

CNRS, Université de Bordeaux, ICMCB, Site ENSCPB, 87 Av. Dr A. Schweitzer, 33608 PESSAC Cedex, France, Centre de Ressources en Microscopie Electronique et Microanalyse, Université Bordeaux I, 351 cours de la Libération, 33405 Talence, France, and SAFT, Direction de la Recherche, 111-113 Bld A. Daney, 33000 Bordeaux, France

Received February 14, 2007. Revised Manuscript Received May 16, 2008

$Li_y(Ni_{0.425}Mn_{0.425}Co_{0.15})_{0.88}O_2$ materials were synthesized by a slow rate electrochemical deintercalation from $Li_{1.12}(Ni_{0.425}Mn_{0.425}Co_{0.15})_{0.88}O_2$ during the first charge and the first discharge in order to study the structural modifications occurring during the first cycle and especially during the irreversible "plateau" observed in charge at 4.5 V vs Li^+/Li. Chemical Li titrations showed that the lithium ions are actually deintercalated from the material during the entire first charge process, excluding the possibility that electrolyte decomposition causes the "plateau". Redox titrations revealed that the average transition metal oxidation state is almost constant during the "plateau", despite further lithium ion deintercalation. ^1H MAS NMR data showed that no Li^+/H^+ exchange was associated to the "plateau" itself. Rietveld refinement of the XRD pattern for a material reintercalated after being deintercalated at the end of the "plateau", as well as redox titrations, revealed an M/O ratio larger than that of the pristine material, which is consistent with the oxygen loss proposed by Dahn and coauthors for the $LiNi_xLi_{(1/3-2x/3)}Mn_{(2/3-x/3)}O_2$ materials to explain the irreversible overcapacity phenomenon observed upon overcharge. X-ray and electron diffraction showed that the transition metal ordering initially present within the slabs is lost during the "plateau" due to a cation redistribution. To explain this behavior a cation migration to the vacancies formed by the lithium deintercalation from the transition metal sites (3a) is assumed, leading to a material densification.

Introduction

As an attempt to replace $LiCoO_2$ currently used as positive electrode in lithium-ion batteries, $LiMnO_2$ was proposed as a promising candidate [1–3] However, this compound was found to suffer from a poor capacity retention due to an evolution to the spinel structure upon cycling.[4–7] Nevertheless, interest was recently focused on the layered manganese-rich $LiNi_xLi_{(1/3-2x/3)}Mn_{(2/3-x/3)}O_2$ materials that can be considered as a partial substitution of Ni for Mn and Li in Li_2MnO_3. Indeed, because of the presence of manganese ions only at the tetravalent state, these compounds, which do not convert into spinel during cycling, were shown to exhibit a higher reversible capacity with an excellent cycling stability and better safety characteristics than $LiCoO_2$.[8–13] From a structural point of view, ^6Li magic angle spinning nuclear magnetic resonance (MAS NMR) showed the presence of Li ions in the Ni/Mn layers in the $LiNi_xLi_{(1/3-2x/3)}Mn_{(2/3-x/3)}O_2$ materials;[14] these results indicated that Li ions present in the Ni/Mn layers are preferentially surrounded by Mn^{4+} ions, leading to a cation ordering in the slab. Further ^6Li MAS NMR experiments on the deintercalated $Li_yNi_xLi_{(1/3-2x/3)}Mn_{(2/3-x/3)}O_2$ phases revealed that these Li ions participate in the electrochemical processes.[15] In $LiNi_xLi_{(1/3-2x/3)}Mn_{(2/3-x/3)}O_2$, the Ni and Mn ions are in the divalent and tetravalent oxidation states, respectively. X-ray absorption near-edge spectroscopy (XANES) data showed that lithium deintercalation from such materials is associated to the oxidation of Ni^{2+} into Ni^{4+} ions, the manganese ions

* Corresponding author. Tel.:+33-5-4000-2647(ICMCB) or +33-5-4000-2234(ENSCPB); Fax: +33-5-4000-6698, E-mail: laurence.croguennec@icmcb-bordeaux.cnrs.fr.

[†] CNRS, Université de Bordeaux, ICMCB, Site ENSCPB.

[‡] Centre de Ressources en Microscopie Electronique et Microanalyse, Université Bordeaux I.

[§] SAFT.

(1) Ohzuku, T.; Ueda, A.; Hirai, T. *Chem. Express* **1992**, *7*, 193.
(2) Davidson, I. J.; McMillan, R. S.; Murray, J. J.; Greedan, J. E. *J. Power Sources* **1995**, 232.
(3) Paulsen, J. M.; Dahn, J. R. *The 1999 Joint International Meeting*; Hawaii, 1999; Vol. 99-2.
(4) Bruce, P. G.; Armstrong, A. R.; Gitzendanner, R. L. *J. Mater. Chem.* **1999**, *9*, 193.
(5) Capitaine, F.; Gravereau, P.; Delmas, C. *Solid State Ionics* **1996**, *89*, 197.
(6) Croguennec, L.; Deniard, P.; Brec, R. *J. Electrochem. Soc.* **1997**, *144*, 3323.
(7) Reed, J.; Ceder, G.; Van Der Ven, A. *Electrochem. Solid State Lett.* **2001**, *4*, A78.
(8) Lu, Z. H.; MacNeil, D. D.; Dahn, J. R. *Electrochem. Solid State Lett.* **2001**, *4*, A191.
(9) Lu, Z. H.; Dahn, J. R. *J. Electrochem. Soc.* **2002**, *149*, 815.
(10) Park, Y. J.; Hong, Y. S.; Wu, X. L.; Ryu, K. S.; Chang, S. H. *J. Power Sources* **2004**, *129*, 288.
(11) Yu, L. H.; Cao, Y. L.; Yang, H. X.; Ai, X. P.; Ren, Y. Y. *Mater. Chem. Phys.* **2004**, *88*, 353.
(12) Lee, C. W.; Sun, Y. K.; Prakash, J. *Electrochim. Acta* **2004**, *49*, 4425.
(13) Sun, Y. K.; Kim, M. G.; Kang, S. H.; Amine, K. *J. Mater. Chem.* **2003**, *13*, 319.
(14) Yoon, W. S.; Iannopollo, S.; Grey, C. P.; Carlier, D.; Gorman, J.; Reed, J.; Ceder, G. *Electrochem. Solid State Lett.* **2004**, *7*, A167.
(15) Grey, C. P.; Yoon, W. S.; Reed, J.; Ceder, G. *Electrochem. Solid State Lett.* **2004**, *7*, A290.

10.1021/cm070435m CCC: $40.75
Published on Web 07/15/2008

remaining at the tetravalent state.[16] Note also that a very careful study of the structural changes occurring upon cycling for $Li_yNi_{1/2}Mn_{1/2}O_2$ ($x = 1/2$ in $LiNi_xLi_{(1/3-2x/3)}Mn_{(2/3-x/3)}O_2$) was recently reported by Breger et al.:[17] they showed using a combination of neutron diffraction, ^{6}Li MAS NMR, electrochemistry, and first principles calculations that the nickel ions from the lithium layers move to the transition metal sites vacated by lithium upon charging above 4.5 V vs Li^+/Li. This cation migration is reversible, at least partially.

In lamellar systems, it is usually accepted that the charging process ends when all the transition metal ions are in the tetravalent oxidation state: surprisingly, a further charging process occurred for the most overlithiated $LiNi_xLi_{(1/3-2x/3)}Mn_{(2/3-x/3)}O_2$ materials beyond the theoretical tetravalent state of the transition metal ions. The voltage profile is characterized by a long and irreversible domain, where the potential is almost constant at 4.5 V vs Li^+/Li (i.e., a "plateau"). Lu and Dahn hypothesized that this irreversible overcapacity could be explained by simultaneous Li and oxygen extraction during the "plateau".[9] From the analysis of the X-ray diffraction (XRD) data by the Rietveld method, they proposed the formation of oxygen vacancies for the materials charged up to 4.8 V. Bruce and Robertson suggested also that this "plateau" was not only explained by an oxygen loss but also by some Li^+/H^+ exchange, the latter being generated from the electrolyte decomposition at high voltage.[18] Similar "plateaus" were observed for other overlithiated lamellar compounds such as $Li[Co_xLi_{(1/3-x/3)}Mn_{(2/3-2x/3)}]O_2$, $Li[Cr_xLi_{(1/3-x/3)}Mn_{(2/3-2x/3)}]O_2$, and $Li_x[Mn_{1-y}Li_y]O_2$,[19–23] suggesting that these electrochemical characteristics are linked to overlithiation (general formula: $Li(Li_yM_{1-y})O_2$).[24]

Some of us reported on the structure of $LiNi_{0.425}Mn_{0.425}Co_{0.15}O_2$ (Li/M ratio equal to 1) and showed an exchange between Li^+ ions from the interslab space and Ni^{2+} ions from the slab, resulting in the presence of about 0.08 Li^+ ions in the slab by the Rietveld refinement of its X-ray and neutron diffraction data.[25,26] A smooth voltage profile, without any "plateau", could be observed in the 2−4.5 V range. This result is in agreement with those obtained for $LiNi_{1/2}Mn_{1/2}O_2$ that does not exhibit any "plateau" in the 2−4.5 V potential range despite ~0.08 Li^+ in the slab.[27,28] More recently, we reported on the structure and the electrochemical behavior of the overlithiated $Li_{1+x}(Ni_{0.425}Mn_{0.425}Co_{0.15})_{1-x}O_2$ materials (i.e., with a Li/M ratio larger than 1).[29] A smooth profile of the battery cycling curve was observed for all the materials in the 2−4.3 V potential range, with a decreasing reversible capacity with overlithiation, which is in good agreement with the decreasing number of exchangeable electrons. Indeed, it was found that the amount of Ni^{3+} ions increases in $Li_{1+x}(Ni_{0.425}Mn_{0.425}Co_{0.15})_{1-x}O_2$ with overlithiation (x) for charge compensation. When the cells are charged to higher voltages, an irreversible "plateau" whose length increases with overlithiation is observed, as shown in Figure 1 by a comparison of first charge curves obtained for $Li//Li_{1+x}(Ni_{0.425}Mn_{0.425}Co_{0.15})_{1-x}O_2$ cells (with $x = 0$, 0.03, 0.08, and 0.12).[8,29] As also shown in Figure 2a for $Li_{1.12}(Ni_{0.425}Mn_{0.425}Co_{0.15})_{0.88}O_2$, after the "plateau" there is an increase of the reversible capacity (120 mA h/g vs 110 mA h/g) in the 2−4.3 V range and of the polarization (100 mV vs 50 mV). Moreover, as shown in Figure 2b, the average potential decreases and the discharge ends more smoothly after the "plateau". The formation of oxygen vacancies in the bulk suggested by Lu and Dahn to explain what was occurring on the high voltage "plateau" is difficult to understand from a physical point of view:[9] how can O^{2-} ions be extracted from an fcc oxygen packing at room temperature without any modification of the material crystallinity? We made the hypothesis of an oxygen loss at the particle surface, followed by a cation migration from the surface to the bulk thanks to vacancies formed upon deintercalation of the lithium ions which were initially present in the $(Li,Ni,Mn,Co)O_2$ slabs. This hypothesis, supported by experimental results, was previously reported.[30] Very recently Armstrong et al. confirmed this hypothesis using in situ differential electrochemical mass spectrometry.[31]

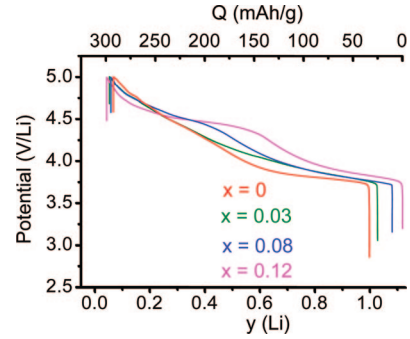

Figure 1. Comparison of the first charge curves obtained for $Li//Li_{1+x}(Ni_{0.425}Mn_{0.425}Co_{0.15})_{1-x}O_2$ cells ($x = 0$, 0.03, 0.08, and 012) at a C/20 rate and with a cutoff voltage of 5.0 V. The liquid electrolyte used in these lithium cells was $LiPF_6$ (1 M) in PC/EC/DMC (1/1/3).

(16) Yoon, W.; Paik, Y.; Yang, X.; Balasubramanian, M.; McBreen, J.; Grey, C. *Electrochem. Solid State Lett.* **2002**, *5*, A263.
(17) Bréger, J.; Meng, Y. S.; Hinuma, Y.; Kumar, S.; Kang, K.; Shao-Horn, Y.; Ceder, G.; Grey, C. *Chem. Mater.* **2006**, *18*, 4768–4781.
(18) Robertson, A. D.; Bruce, P. G. *Electrochem. Solid State Lett.* **2004**, *7*, A294.
(19) Park, Y. J.; Hong, Y. S.; Wu, X. L.; Kim, M. G.; Ryu, K. S.; Chang, S. H. *J. Electrochem. Soc.* **2004**, *151*, A720.
(20) Grincourt, Y.; Storey, C.; Davidson, I. J. *J. Power Sources* **2001**, *97−98*, 711. (Special Issue)
(21) Storey, I.; Kargina, Y.; Grincourt, I. J.; Davidson, Y. C.Yoo.; Seung, D. Y. *J. Power Sources* **2001**, *97−98*, 541. (Special Issue)
(22) Ammundsen, B.; Paulsen, J.; Davidson, I.; Liu, R. S.; Shen, C. H.; Chen, J. M.; Jang, L. Y.; Lee, J. F. *J. Electrochem. Soc.* **2002**, *149*, A431.
(23) Armstrong, A. R.; Bruce, P. G. *Electrochem. Solid State Lett.* **2004**, *7*, A1.
(24) Park, K. S.; Cho, M. H.; Jin, S. J.; Nahm, K. S.; Hong, Y. S. *Solid State Ionics* **2004**, *171*, 141.
(25) Tran, N. Ph.D. thesis, University Bordeaux I, 2005.
(26) Tran, N.; Croguennec, L.; Jordy, C.; Biensan, P.; Delmas, C. *Solid State Ionics* **2005**, *176*, 1539.
(27) Shaju, K. M.; Rao, G. V. S.; Chowdari, B. V. R. *Electrochim. Acta* **2004**, *49*, 1565.
(28) Grey, C. P.; Dupre, N. *Chem. Rev.* **2004**, *104*, 4493.
(29) Tran, N.; Croguennec, L.; Labrugère, C.; Jordy, C.; Biensan, P.; Delmas, C. *J. Electrochem. Soc.* **2006**, *153*, A261−A269.
(30) Croguennec, L.; Tran, N.; Weill, F.; Ménétrier, M.; Delmas, C. *Lithium Battery Discussions - Electrode Materials*, Bordeaux, Arcachon, France, 22−27 May, 2005; Extended Abstract no. T47, p 222.
(31) Armstrong, A. R.; Holzapfel, M.; Novák, P.; Johnson, C. S.; Kang, S.-H.; Thackeray, M. M.; Bruce, P. G. *J. Am. Chem. Soc.* **2006**, *128*, 8694.

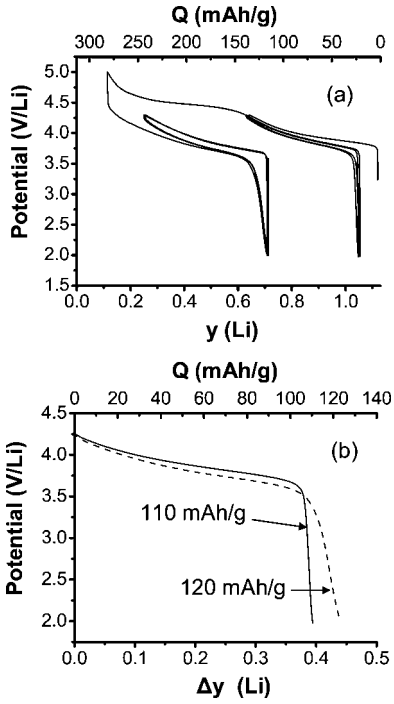

Figure 2. (a) Charge−discharge curve of a Li//$Li_{1.12}(Ni_{0.425}Mn_{0.425}Co_{0.15})_{0.88}O_2$ cell at a constant C/20 rate: in the 2−4.3 V range for two cycles, then in the 2−5.0 V for one cycle, and again for two cycles in the 2−4.3 V range. (b) Comparison of the discharge curves in the 2−4.3 V range before (solid) and after (dashed) the "plateau". The liquid electrolyte used in these lithium cells was $LiPF_6$ (1 M) in PC/EC/DMC (1/1/3).

A detailed study of the mechanisms involved from a structural and redox point of view on the "plateau" is presented in this paper. A ^1H MAS NMR study is also reported in order to decide if for these materials a Li^+/H^+ ion exchange occurs during the "plateau".

Experimental Section

Synthesis of the Base Material $Li_{1.12}(Ni_{0.425}Mn_{0.425}Co_{0.15})_{0.88}O_2$. $Ni(NO_3)_2 \cdot 6H_2O$ (97% Prolabo), $Mn(NO_3)_2 \cdot 4H_2O$ (98% Fluka), $Co(NO_3)_2 \cdot 6H_2O$ (98% Prolabo), LiOH (98+ % Alfa Aesar), and NH_4OH (28−30% J.T. Baker) were used as starting materials. The $Li_{1.12}(Ni_{0.425}Mn_{0.425}Co_{0.15})_{0.88}O_2$ material was prepared using the coprecipitation method.[32] A mixed (1 M) aqueous solution of $Ni(NO_3)_2$, $Mn(NO_3)_2$, and $Co(NO_3)_2$ prepared with the 42.5/42.5/15 molar ratio was added dropwise by a buret into a basic solution (LiOH (1 M)/NH_4OH (3 M)) under magnetic stirring. Note that the initial Li/(Ni + Co + Mn) ratio was adjusted to 1.20/0.80. A green-brown mixed hydroxide precipitated. Water was removed by evaporation at 80 °C under primary vacuum using a rotavapor device. The resulting wet precipitate was dried overnight at 105 °C, precalcined at 500 °C for 5 h in air, and then calcined at 1000 °C for 12 h in air in a tubular furnace. The heating up speed was fixed to 5 °C/min, and the cooling down speed was fixed to 4 °C/min.

Electrochemical Preparation of the $Li_y(Ni_{0.425}Mn_{0.425}Co_{0.15})_{0.88}O_2$ Samples. The electrochemical deintercalation was carried out in a two electrode test cell using lithium as the negative electrode. The positive electrodes consisted of a mixture of 90 wt % of active material and 10 wt % of carbon black/graphite (1:1); no binder was used, but the positive electrode mixture was pressed in order to have a good electronic contact between the grains to minimize cell polarization. $LiPF_6$ (1 M) dissolved in a mixture of propylene carbonate (PC), ethylene carbonate (EC), and dimethyl carbonate (DMC) (1:1:3 by volume) was used as electrolyte. The cells were assembled and cycled using a homemade system at room temperature in an argon-filled dry box; a slow cycling rate (C/300, with C corresponding to a theoretical exchange of one electron in 1 h during charge) was used in galvanostatic mode, with alternating periods of relaxation in order to be close to the thermodynamic equilibrium. When the target lithium compositions were reached, the positive electrodes were removed from the cells, washed with DMC, and then dried under vacuum at room temperature.

Chemical Analyses and Redox Titration. The Li content in the materials was analyzed using atomic absorption spectroscopy (AAS) in emission mode. The average mass percentage of the transition metal ions was checked by complexometric titration: after dissolution of the samples in HCl (37%), the solution was neutralized with an ammonia solution and then titrated with EDTA in the presence of ascorbic acid and of murexid as a coloring agent. The average oxidation state of the transition metal ions was determined by iodometric titration: the samples were hydrothermally dissolved at 40 °C overnight in an aqueous solution of HCl and KI; then the resulting solution was titrated with $Na_2S_2O_3$ (0.01 M). Note that the whole process including sample dissolution was carried out at least twice and that a good reproducibility of the results was achieved.

^1H MAS NMR Experimental Conditions. ^1H MAS NMR experiments were performed using a Bruker Avance 300 spectrometer with a 10 kHz spinning speed. A standard Bruker MAS probe was used with 4 mm diameter zirconia rotors, the materials being mixed with dry silica in the 1: 1 weight ratio in order to facilitate the spinning and to improve the field homogeneity, as the analyzed materials can have paramagnetic or metallic properties. The rotors were filled in an argon filled glovebox. A Hahn Echo sequence was used to allow the observation of possible very broad signals. The 90° pulse duration was 2.4 μs, and the time between two successive pulses was 100 μs (one rotor period). The spectral width was 500 kHz. The time between two scans (2000 scans per spectrum) was fixed to 2 s, which was sufficient to prevent the signal saturation. The isotropic shifts, expressed in ppm, are referenced to an aqueous solution of tetramethylsilane (TMS).

XRD Analysis. The materials were analyzed by XRD using a Siemens D5000 diffractometer equipped with a diffracted-beam monochromator (Cu Kα radiation) in the 10−110° ($2\theta_{Cu}$) range in steps of 0.02° ($2\theta_{Cu}$) with a constant counting time of 15 s. As the materials were recovered from electrodes, a hygroscopic sample-holder was used to prevent any contact of the material with room atmosphere and thus to avoid any evolution of these metastable phases. The profile matching and the Rietveld refinement of the data were performed using the Fullprof software.[33]

Magnetic Properties Analysis. Magnetic measurements were carried out with a Superconducting Quantum Interference Device (quantum design MPMS-5S). Magnetization vs field plots were recorded at 5 K over the [−2000 Oe; +2000 Oe] range.

Electron Diffraction Analysis. For the electron diffraction experiments, a JEOL 2000FX microscope, equipped with a double tilt specimen stage, was used at an accelerating voltage of 200 kV. Previous to the observation, a suspension was obtained by grinding the materials in ethanol, a droplet of this suspension being deposited on a carbon grid.

(32) Caurant, D.; Baffier, N.; Garcia, B.; Pereira-Ramos, J. P. *Solid State Ionics* **1996**, *91*, 45.

(33) Rodriguez-Carvajal, J. Laboratoire Léon Brillouin. http://www-llb-.cea.fr/fullweb/powder.htm (2004).

Table 1. Experimental Li Content ($y_{titr.}$) Obtained by Chemical Analysis of the $Li_y(Ni_{0.425}Mn_{0.425}Co_{0.15})_{0.88}O_2$ Materials Recovered at Target Values ($y_{elec.}$ = 1.12, 0.78, 0.54, 0.22, 0.93, 0.73)

$y_{elec.}$	$y_{titr.}$	comment
1.12	1.12	pristine material
0.78	0.83	obtained during the first charge
0.54	0.60	obtained during the first charge
0.22	0.30	obtained during the first charge
0.93	0.98	obtained during the first discharge after a charge just before the "plateau" (up to $y_{elec.}$ = 0.54)
0.73	0.70	obtained during the first discharge after a charge on the "plateau" (up to $y_{elec.}$ = 0.22)

Table 2. Experimental Average Oxidation State (oxid. state$_{(titrated)}$) Obtained by Iodometric Titration for the $Li_y(Ni_{0.425}Mn_{0.425}Co_{0.15})_{0.88}O_2$ ($y_{elec.}$ = 1.12, 0.78, 0.54, 0.22) Materials[a]

$y_{elec.}$	oxid. state$_{(titrated)}$	oxid. state$_{(calculated)}$
1.12	3.25	3.27
0.78	3.60	3.60
0.54	3.86	3.86
0.22	3.89	4.20[b]

[a] Comparison with the theoretical ones (oxid. state$_{(calculated)}$) calculated based on the actual amount of lithium ions remaining in the material ($y_{titr.}$) after deintercalation. [b] Average oxidation state assumed based on a possible oxidation of manganese ions beyond the tetravalent state.

Results

The $Li_y(Ni_{0.425}Mn_{0.425}Co_{0.15})_{0.88}O_2$ ($y_{elec.}$ = 0.22, 0.54, 0.78; $y_{elec.}$ being the composition based on the number of exchanged electrons) phases were obtained by electrochemical lithium deintercalation from $Li_{1.12}(Ni_{0.425}Mn_{0.425}Co_{0.15})_{0.88}O_2$. The $Li_y(Ni_{0.425}Mn_{0.425}Co_{0.15})_{0.88}O_2$ ($y_{elec.}$ = 0.73, 0.93) phases were obtained by discharge of Li//$Li_{1.12}(Ni_{0.425}Mn_{0.425}Co_{0.15})_{0.88}O_2$ cells down to 3.2 V after a charge to a lithium composition of $y_{elec.}$ = 0.22 and $y_{elec.}$ = 0.54, respectively. These materials were analyzed by several techniques as it will be detailed in the following.

1. Chemical Li Titrations. In order to confirm that the excess of capacity observed after the oxidation of all the transition metal ions to the tetravalent state was not due to a side reaction such as the electrolyte decomposition only, the Li content in the $Li_y(Ni_{0.425}Mn_{0.425}Co_{0.15})_{0.88}O_2$ ($y_{elec.}$ = 1.12, 0.78, 0.54, 0.22, 0.93, 0.73) materials was titrated by AAS. As shown in Table 1, the experimental lithium concentration values were found to be rather close to those expected from the number of exchanged electrons. This clearly shows also that lithium ions are really deintercalated from $Li_{1.12}(Ni_{0.425}Mn_{0.425}Co_{0.15})_{0.88}O_2$ even over the range where the average transition metal oxidation state was theoretically already 4+, excluding that the "plateau" could be only due to side reactions like electrolyte decomposition at the electrode surface, which would not involve the positive electrode material itself.

2. Redox Titrations. The experimental average transition metal oxidation states obtained for the $Li_y(Ni_{0.425}Mn_{0.425}Co_{0.15})_{0.88}O_2$" ($y_{elec.}$= 1.12, 0.78, 0.54, 0.22) materials by iodometric titration assuming the $Li_yM_{0.88}O_2$ formula are reported in Table 2 and compared to the theoretical ones calculated from the actual lithium amount remaining in each material ($y_{titr.}$). One can observe a good agreement between the experimental transition metal oxidation states and the theoretical ones except for the material obtained at the end of the "plateau" ($y_{elec.}$= 0.22): if we assume possible oxidation of the manganese ions beyond the tetravalent state, a theoretical oxidation state of 4.20 is expected for this material. An experimental value of 3.89 was actually obtained, which indicated first that the average oxidation state was almost constant on the "plateau" (the variation being within the accuracy of the titration), then that the manganese ions would remain at the tetravalent state, and finally that the Co^{3+} ions would not be fully oxidized during the "plateau", at least until the $y_{elec.}$= 0.22 lithium composition. Similar results were also recently reported by Choi and Manthiram for $LiNi_{1/3}Mn_{1/3}Co_{1/3}O_2$.[34] No significant change of the average transition metal oxidation state was thus observed on the "plateau" despite the further lithium deintercalation from the material: this is in good agreement with the two hypotheses proposed by other authors to explain this overcapacity phenomenon: (i) the removal of lithium compensated for by an oxygen loss[9] and/or (ii) an exchange reaction between Li^+ and H^+, this latter being generated by the electrolyte oxidation.[18]

3. ^{1}H MAS NMR. In order to determine whether or not the Li^+/H^+ exchange mechanism can be partially associated to the "plateau", as proposed by Bruce et al.,[18] $Li_y(Ni_{0.425}Mn_{0.425}Co_{0.15})_{0.88}O_2$ materials obtained during the first charge were analyzed by ^{1}H MAS NMR which allows the direct characterization of inserted protons in these materials.

Several $Li_y(Ni_{0.425}Mn_{0.425}Co_{0.15})_{0.88}O_2$ materials with a lithium composition close to $y_{elec.}$ = 0.3 (i.e., obtained on the "plateau") were synthesized by slow electrochemical deintercalation at a constant C/300 rate. The ^{1}H MAS NMR spectra associated to these four samples are reported in Figure 3. All of them show one signal not shifted (i.e., at 0 ppm) and split into spinning side bands, which is associated to protons adsorbed at the material surface and two other signals at ±30 ppm corresponding to surface MOH type defects. Probe artifacts also contribute to these signals. Nevertheless, significant differences can be observed between these spectra in the intensity of a very broad signal. The lithium contents given by the electrochemical curve ($y_{elec.}$) and by the chemical titrations ($y_{titr.}$) are also reported in Figure 3. More or less significant differences (noted Δy) were found between these ($y_{elec.}$) and ($y_{titr.}$) values; nevertheless, it is essential to keep in mind that most of the materials obtained on the "plateau" showed Δy values close to zero. Note that the larger the difference (Δy) between $y_{elec.}$ and $y_{titr.}$, the higher was the intensity of the very broad signal in the ^{1}H MAS NMR spectrum. This is explained, in the case of samples A and B, by parasitic electrolyte decomposition at high potential, as revealed by an erratic voltage on the charge curves around 4.5 V instead of the smooth curves shown in Figures 1 and 2 (see Supporting Information, Figure S1). Indeed, electrolyte degradation produces protons that must be exchanged with lithium into the materials afterward (see Supporting Information, Figure S2, for the assignment of this broad signal due to very strong dipolar interaction with the electron spins carried by Ni and Mn). This establishes that protons present in the material (from parasitic electrolyte decomposition) are observed by ^{1}H MAS NMR in our experimental conditions.

(34) Choi, J.; Manthiram, A. *J. Electrochem. Soc.* **2005**, *152*, A1714.

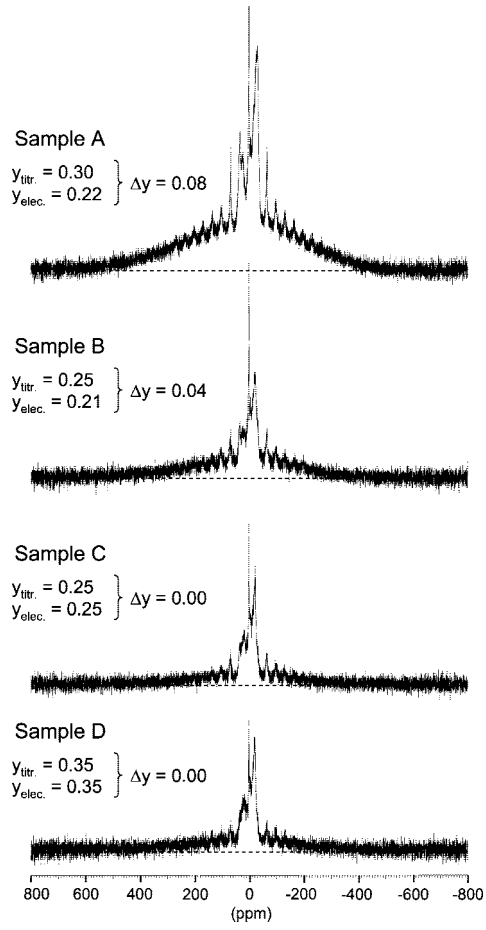

Figure 3. ^{1}H MAS NMR spectra recorded in Echo conditions at 10 kHz for the $Li_y(Ni_{0.425}Mn_{0.425}Co_{0.15})_{0.88}O_2$ materials (samples A−D synthesized electrochemically in a lithium cell cycled at a C/300 rate). A comparison between the experimental Li content ($y_{titr.}$) obtained by chemical analysis and the electrochemically target value ($y_{elec.}$) is given for each $Li_y(Ni_{0.425}Mn_{0.425}Co_{0.15})_{0.88}O_2$ material.

Comparison between the ^{1}H MAS NMR spectrum of the pristine material ($y = 1.12$), that of a material deintercalated before the "plateau" ($y_{elec.} = 0.78$) and that of a material ($y_{elec.} = 0.35$, sample D) representative of the materials deintercalated on the "plateau" when no additional parasitic electrolyte decomposition occurs, is reported in Figure 4 and shows that no proton insertion occurs during the first charge and especially during the "plateau". In the present study it can therefore be concluded that H^+/Li^+ exchange, when it occurs, is only a parasitic side reaction: the mechanism intrinsic to the "plateau" observed during the first charge at high potential does not involve any proton insertion in the positive electrode material.

4. XRD. Figure 5a shows the XRD patterns of the $Li_y(Ni_{0.425}Mn_{0.425}Co_{0.15})_{0.88}O_2$($y_{elec.} = 0.78$, 0.54, 0.22) materials obtained during the first charge, compared with that of the pristine material ($y = 1.12$). All the peaks could be indexed based on a hexagonal α-$NaFeO_2$ type structure, except those in the 20−25° (2θ) range. As shown in Figure 5c, the splitting of the (018)/(110) doublet clearly increases up to the beginning of the "plateau" (i.e., up to $y_{elec.} = 0.54$) and seems to remain constant through the "plateau", suggesting an insignificant evolution of the lattice parameters in the $0.22 < y_{elec.} < 0.54$ lithium composition range.

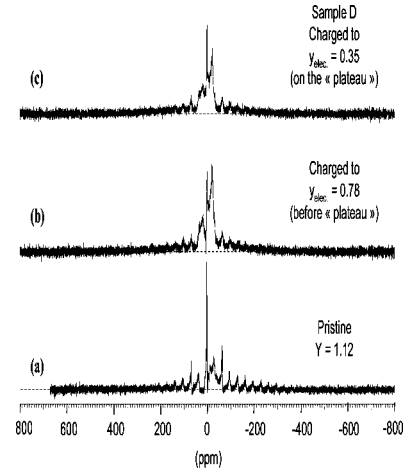

Figure 4. ^{1}H MAS NMR spectra recorded in echo conditions at 10 kHz for (a) the pristine material ($y = 1.12$), (b) a material obtained in the first charge and deintercalated before the "plateau" ($y_{elec.} = 0.78$), and (c) a material ($y_{elec.} = 0.35$, Sample D) that is representative of most of the materials obtained in the first charge and deintercalated on the "plateau".

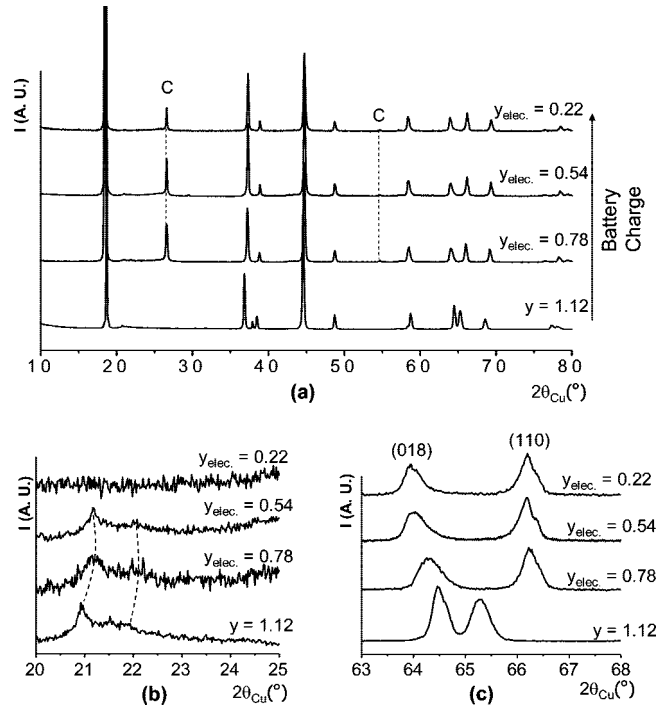

Figure 5. (a) XRD patterns of the $Li_y(Ni_{0.425}Mn_{0.425}Co_{0.15})_{0.88}O_2$ ($y_{elec.} =$ 0.78, 0.54, 0.22) materials obtained during the first charge, compared with that of the pristine material ($y = 1.12$); detailed XRD data in the 20−25° ($2\theta_{Cu}$) range (b) and in the 63−68° ($2\theta_{Cu}$) range (c). The graphite diffraction lines are indicated by "C".

The XRD pattern of the pristine material exhibits superlattice peaks in the 20−25° (2θ) range due to an in-plane cation ordering between the Li, Ni, Mn, and Co ions among two α and β sites in the transition metal layers, as explained in detail in ref 35 (Figure 5b). Interestingly these superlattice peaks decrease in intensity in the $0.22 < y_{elec.} < 0.54$ lithium composition range (i.e., on the "plateau") and are not detected anymore for the material charged up to the end of the "plateau" ($y_{elec.} = 0.22$), as also observed by Hong et al. for

(35) Weill, F.; Tran, N.; Croguennec, L.; Delmas, C. *J. Power Sources* **2007**, *172*, 893.

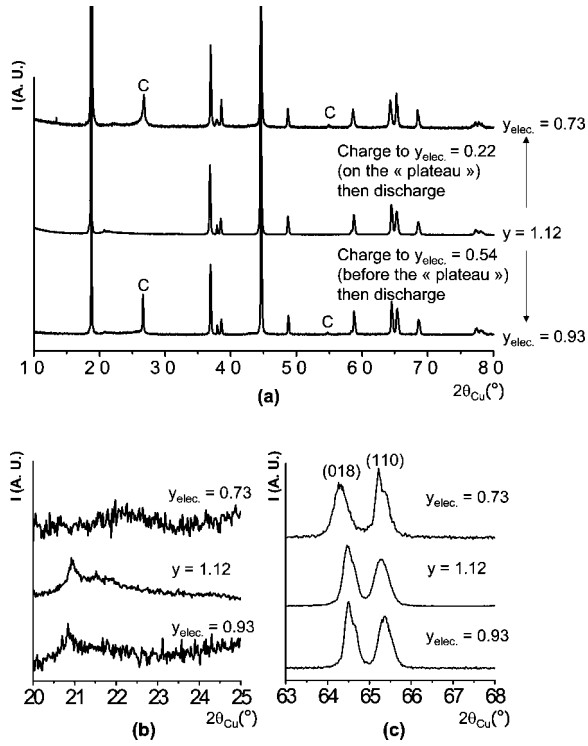

Figure 6. (a) XRD patterns of the $Li_y(Ni_{0.425}Mn_{0.425}Co_{0.15})_{0.88}O_2$ ($y_{elec.}$ = 0.93, 0.73) materials obtained at the end of the first discharge after a charge before and after the "plateau", respectively; the patterns were compared with that of the pristine material (y = 1.12); detailed XRD data in the 20−25° ($2\theta_{Cu}$) range (b) and in the 63−68° ($2\theta_{Cu}$) range (c) are also given. The graphite diffraction lines are indicated by "C".

Li_2MnO_3, $Li[Ni_{0.20}Li_{0.20}Mn_{0.60}]O_2$, and $Li[Co_{0.20}Li_{0.27}Mn_{0.53}]O_2$.[36] This suggests a loss of the in-plane cation ordering within the slab during the "plateau".

As shown in Figure 6 a−c, the XRD pattern of the material reintercalated after a charge at the beginning of the "plateau" ($y_{elec.}$ = 0.93) seems very similar to that of the pristine material (y = 1.12), based, for instance, on the (018)/(110) doublet intensity ratio and on the presence of the superlattice peaks in the 20−25° (2θ) range. In contrast, no superlattice peak can be observed and the (018)/(110) doublet is different in position and in intensity in the XRD pattern of the material reintercalated after a charge at the end of the "plateau" ($y_{elec.}$ = 0.73). This suggests that the cation ordering present in the slab for the pristine material is irreversibly lost during the "plateau", which was recently confirmed by an electron diffraction study.[37] Note that a peak and a large bump with a very low intensity are observed at 14° (2θ) and 22.5° (2θ), respectively, for the $Li_{0.73}(Ni_{0.425}Mn_{0.425}Co_{0.15})_{0.88}O_2$ material, but they were not clearly reproducible and were therefore not explained.

4.1. Cell Parameters Evolution. Analyses of the XRD data were performed assuming an α-$NaFeO_2$ type structure ($R\bar{3}m$ space group). The lattice parameters versus lithium composition (that obtained from the chemical titrations) for the deintercalated and the reintercalated phases are given in Table 3. Figure 7 shows the lattice parameters evolution versus lithium composition for $Li_{1.12}(Ni_{0.425}Mn_{0.425}Co_{0.15})_{0.88}O_2$, in comparison with that of $LiNiO_2$.[38]

Upon charging to the ($y_{titr.}$ = 0.60) lithium composition, the $a_{hex.}$ parameter decreased and the $c_{hex.}$ parameter clearly increased. Indeed, in the early stages of deintercalation the oxidation of the transition metal ions implies a decrease of the metal−oxygen distance leading to a decrease of the $a_{hex.}$ parameter. Note that this decrease is less pronounced than that observed for $LiNiO_2$: it could be attributed to the formation of lithium vacancies in the slab for $Li_{1.12}(Ni_{0.425}Mn_{0.425}Co_{0.15})_{0.88}O_2$, which occurs only in this composition range. Indeed the formation of a cation vacancy in the slab leads to an effect opposite to a cation oxidation. Furthermore, upon deintercalation the lithium ions do not play their role of screening ions anymore, leading to stronger repulsions between the oxygen layers localized on both sides of the interslab space and thus to an increase of the $c_{hex.}$ parameter.

In the 0.30 < $y_{titr.}$ < 0.60 range (i.e., on the "plateau"), the variation in the lattice parameters is significantly reduced vs that already observed for the $LiNiO_2$ system suggesting that a different behavior occurs. The almost constant value observed for the $a_{hex.}$ parameter shows that there is no cation oxidation in that lithium composition range, in good agreement with redox titrations. Concerning the $c_{hex.}$ parameter, from a general point of view its variation results from the competition between the oxygen−oxygen repulsion when the lithium ions are deintercalated and the strong change in the M−O bond covalency due to the transition metal oxidation. The relatively small variation observed in this case shows that the change in covalency is not predominant, in agreement with the almost constant average oxidation state for the transition metal ions.

Note that in the 0.10 < $y_{titr.}$ < 0.30 range, the $a_{hex.}$ parameter surprisingly increased, on the contrary to what is usually observed for the lamellar $Li_y(Ni,M)O_2$ systems.[38–43] The volume variation was very small during the first charge ($\Delta V/V \sim 1\%$), as also observed by Lu et al. for the $Li(Li,Ni,Mn)O_2$ materials.[9]

Concerning the reintercalated phases, their lattice parameters ($a_{hex.}$ and $c_{hex.}$) were found larger than those of the pristine material, especially for $Li_{0.73}(Ni_{0.425}Mn_{0.425}Co_{0.15})_{0.88}O_2$ recovered after the "plateau". It should be highlighted that, without the occurrence of any structural modification of the host structure during the first cycle, the $a_{hex.}$ parameters were expected to remain smaller than that observed for the pristine material.

4.2. Refinement by the Rietveld Method: Structural Analysis. In a previous report,[29] the refinement of the XRD pattern of $Li_{1.12}(Ni_{0.425}Mn_{0.425}Co_{0.15})_{0.88}O_2$ led to the fol-

(36) Hong, Y. S.; Park, Y. J.; Ryu, K. S.; Chang, S. H. *Solid State Ionics* **2005**, *176*, 1035.
(37) Weill, F.; Tran, N.; Martin, N.; Croguennec, L.; Delmas, C. *Electrochem. Solid State Lett.* **2007**, *10* (8), A194.
(38) Croguennec, L.; Pouillerie, C.; Mansour, A. N.; Delmas, C. *J. Mater. Chem.* **2001**, *11*, 131.
(39) Prado, G.; Rougier, A.; Fournès, L.; Delmas, C. *J. Electrochem. Soc.* **2000**, *147* (8), 2880.
(40) Pouillerie, v C.; Croguennec, L.; Delmas, C. *Solid State Ionics* **2000**, *132*, 15.
(41) Croguennec, L.; Suard, E.; Willmann, P.; Delmas, C. *Chem. Mater.* **2002**, *14*, 2149.
(42) Guilmard, M.; Croguennec, L.; Delmas, C. *J. Electrochem. Soc.* **2003**, *150*, A1287.
(43) Guilmard, M.; Rougier, A.; Grüne, M.; Croguennec, L.; Delmas, C. *J. Power Sources* **2003**, *115*, 305.

Table 3. Structural Parameters Determined for the $Li_y(Ni_{0.425}Mn_{0.425}Co_{0.15})_{0.88}O_2$ ($y_{elec.}$ = 1.12, 0.78, 0.54, 0.22, 0.93, 0.73) Materials by the Refinement of Their X-ray Data[a]

$y_{elec.}$	$y_{titr.}$	$a_{hex.}$ (Å)	$c_{hex.}$ (Å)	V (Å^3)	$z_{ox.}$	$S_{(MO_2)}$ (Å)[b]	$I_{(LiO_2)}$ (Å)[c]	M−O (Å)
1.12	1.12	2.8566(5)	14.222(4)	100.5(1)	0.2599(2)	2.09(2)	2.65(2)	1.96(1)
0.78[d]	0.83	2.8293(3)	14.469(4)	100.1(1)				
0.54[d]	0.60	2.8246(3)	14.471(4)	100.4(1)				
0.22[d]	0.30	2.8238(3)	14.476(4)	100.1(1)				
0.93	0.98	2.8583(3)	14.248(2)	100.8(1)	0.2584(6)	2.14(6)	2.61(6)	1.96(1)
0.73	0.70	2.8649(3)	14.327(2)	101.8(1)	0.2613(6)	2.06(6)	2.71(6)	1.95(1)

[a] The standard deviation was multiplied by the Scor parameter to correct for local correlations..[47] [b] Slab thickness: $S_{(MO_2)} = 2(1/3 - z_{ox.})c_{hex.}$; $z_{ox.}$ is the atomic coordinate of oxygen ions. [c] Interslab space thickness: $I_{(LiO_2)} = c_{hex.}/3 - S_{(MO_2)}$. [d] Only a full pattern matching refinement of their XRD data was performed for the materials obtained in charge.

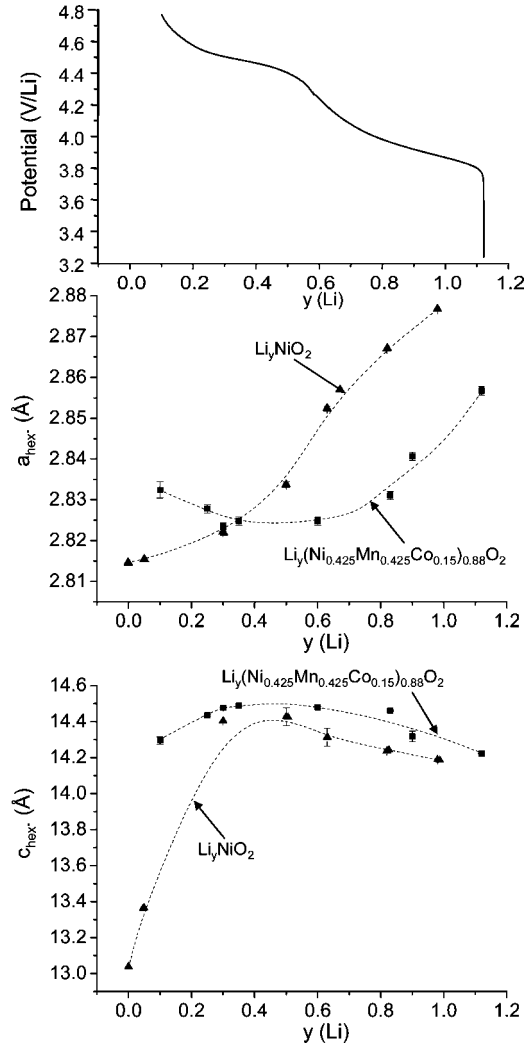

Figure 7. Change of the lattice parameters $a_{hex.}$ and $c_{hex.}$ versus lithium composition ($y_{titr.}$) upon charging for the $Li_{1.12}(Ni_{0.425}Mn_{0.425}Co_{0.15})_{0.88}O_2$ system; the data were compared with those of $LiNiO_2$.[38] The dotted lines are just given as guidelines.

lowing cationic distribution for the pristine material: $(Li_{0.98}Ni_{0.02})_{3b}(Li_{0.14}Ni_{0.354}Mn_{0.374}Co_{0.132})_{3a}O_2$.

For both reintercalated materials, the refinement procedure was carried out in three steps, as described as follows for $Li_{0.73}(Ni_{0.425}Mn_{0.425}Co_{0.15})_{0.88}O_2$: first step, $(Li_{0.70}Ni_{0.02}\square_{0.28})_{3b}(\square_{0.14}Ni_{0.354}Mn_{0.374}Co_{0.132})_{3a}O_2$; second step, $(Li_{0.70}Ni_{0.02+z}\square_{0.28-z})_{3b}(\square_{0.14+z}Ni_{0.354-z}Mn_{0.374}Co_{0.132})_{3a}O_2$, that is, with a possible cation migration between the slab and the interslab space; and third step, $(Li_{0.70}Ni_{0.02+z}\square_{0.28-z})_{3b}(\square_{0.14+z}Ni_{0.354-z}Mn_{0.374}Co_{0.132})_{3a}O_{2-\delta}$, that is, with a possible increase of the M/O ratio and thus an oxygen loss.

In the first step, the Ni ion occupancy in the interslab space was fixed to 0.02, that is, to the value determined for the pristine material. We also assumed the presence of lithium vacancies in the 3a site, in agreement with the results reported by Grey and co-workers for the Li(Li,Ni,Mn)O_2-type materials showing the actual deintercalation of the Li^+ ions from the slab at the early stages of the charge process.[15] The occupancy ratios of the nickel, manganese, and cobalt ions in the 3a site were fixed to 0.354, 0.374, and 0.132, respectively. In the second step, the nickel occupancy in the 3b site was refined in order to take into account a cation migration between the slab and the interslab space that would have possibly occurred in the highly deintercalated state, the total nickel concentration being constrained to 0.374. Note that the choice of the migrating cations from the slab was arbitrary: indeed from XRD only, it is not possible to distinguish between Ni, Co, and Mn, those ions having very similar scattering factors. Indeed, from the solid state chemistry viewpoint, at the end of the charge all these ions would be at the tetravalent state and would have similar ionic radii ($r(Ni^{4+}) = 0.48$ Å; $r(Mn^{4+}) = 0.53$ Å; $r(Co^{4+}) = 0.53$ Å). Furthermore, these three ions would be instable in tetrahedral sites that are the intermediate sites during migration. In the third step, the oxygen ion occupancy was refined to consider an evolution of the M/O ratio and thus a possible oxygen loss.

Structure of the Material That Did Not "See" the High Voltage "Plateau" and Recovered after One Cycle. From the refinement of the XRD data, the formula $(Li_{0.98}Ni_{0.02})_{3b}(\square_{0.14}Ni_{0.354}Mn_{0.374}Co_{0.132})_{3a}O_2$ was shown to describe well the structure of the $Li_{0.93}(Ni_{0.425}Mn_{0.425}Co_{0.15})_{0.88}O_2$ material recovered at the end of the first discharge, following a charge just before the "plateau". Comparison between the experimental and the calculated XRD patterns is given in Figure 8a. A good minimization of the difference is obtained with small reliability factors, both suggesting a good description of the average structure of $Li_{0.93}(Ni_{0.425}Mn_{0.425}Co_{0.15})_{0.88}O_2$ by the model chosen. The nickel occupancy in the lithium site was found to remain equal within the uncertainty to that of the pristine material; moreover, the M/O ratio was found equal to 0.88/2.00(1) as for the pristine material. Note that the theoretical average transition metal oxidation state is 3.43 for $Li_{0.93}(Ni_{0.425}Mn_{0.425}Co_{0.15})_{0.88}O_2$ in good agreement with that determined experimentally from redox titration (oxid. state = 3.45). For $Li_{0.93}(Ni_{0.425}Mn_{0.425}Co_{0.15})_{0.88}O_2$ it appears thus that no significant modification of the structure is observed, as expected

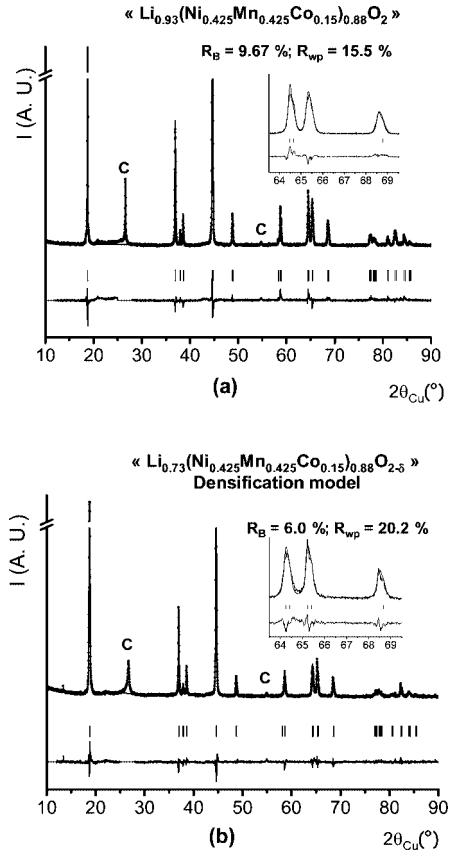

Figure 8. Comparison between the experimental (●) and the calculated (solid line) XRD patterns for (a) $Li_{0.93}(Ni_{0.425}Mn_{0.425}Co_{0.15})_{0.88}O_2$ and for (b) $Li_{0.73}(Ni_{0.425}Mn_{0.425}Co_{0.15})_{0.88}O_{2-\delta}$ with the densification model.

from the good reversibility of the lithium intercalation process when the cycling is performed in the 2.0−4.3 V potential range (Figure 2).

Structure of the Material That Did "See" the High Voltage "Plateau" and Recovered after One Cycle. In contrast, the refinement of the XRD pattern of $Li_{0.73}(Ni_{0.425}Mn_{0.425}Co_{0.15})_{0.88}O_2$ obtained by discharge following a charge up to the end of the "plateau" leads to the cationic distribution $(Li_{0.70}Ni_{0.04}\square_{0.26})_{3b}(\square_{0.16}Ni_{0.334}Mn_{0.374}Co_{0.132})_{3a}O_{1.89}$ and supports thus an oxygen loss. This formula suggests that ∼5.5% of the oxygen ions would be lost upon cycling in the 2.0−5.0 V potential range, with an increase of the M/O ratio from 0.44 for the pristine material to 0.465 for $Li_{0.73}(Ni_{0.425}Mn_{0.425}Co_{0.15})_{0.88}O_{2-\delta}$; an increasing amount of extra-nickel ions in the lithium site (0.04 vs 0.02 initially) was also observed. Note that the increase in the cell polarization observed after the "plateau" in Figure 2 may partially come from this increase in the transition metal occupancy in the Li layers (making ionic diffusion more difficult) when the cell is charged up to the end of the "plateau".

As XRD is not highly sensitive to changes in oxygen contents, it is also interesting to mention that the average oxidation state determined experimentally for the transition metal ions in $Li_{0.73}(Ni_{0.425}Mn_{0.425}Co_{0.15})_{0.88}O_2$ (i.e., 3.39) supports the conclusion of an oxygen loss. Indeed, the theoretical average oxidation state would be 3.75 for the transition metal ions if no oxygen loss occurs, whereas it would be 3.50 if 5.5% oxygen ions are lost from the structure. Note that from the experimental average oxidation state (i.e., 3.39) a larger oxygen loss probably occurred (i.e., $\delta \sim 0.16$ instead of 0.11 as determined by the Rietveld refinement) leading thus to the $(Li_{0.70}Ni_{0.04}\square_{0.26})_{3b}(\square_{0.16}Ni_{0.334}Mn_{0.374}Co_{0.132})_{3a}(O_{1.84}\square_{0.16})_{6c}$ or $(Li_{0.76}Ni_{0.04}\square_{0.20})_{3b}(\square_{0.085}Ni_{0.366}Mn_{0.406}Co_{0.143})_{3a}(O_2)_{6c}$ formula.

Note also that if the oxygen loss (i.e., the $Li_yM_{0.88}O_{1.89}$ formula instead of the $Li_yM_{0.88}O_2$ one) had been taken into account for the chemical Li and redox titrations (Tables 1 and 2), then the correction that should have been applied to the values reported for the materials that have "seen" the "plateau" would have been smaller than the accuracy of the titrations itself.

From the combination of Rietveld refinement of XRD data and redox titration, it was therefore shown that oxygen is lost from the material that did "see" the high voltage "plateau". Note however that the refinement of the XRD data does not allow a structural model with local oxygen vacancies corresponding actually to the distribution $(Li_{0.70}Ni_{0.04}\square_{0.26})_{3b}(\square_{0.16}Ni_{0.334}Mn_{0.374}Co_{0.132})_{3a}(O_{1.89}\square_{0.11})_{6c}$, and that characterized by an oxygen loss followed by a further contraction of the oxygen lattice corresponding to the distribution $(Li_{0.74}Ni_{0.04}\square_{0.22})_{3b}(\square_{0.11}Ni_{0.355}Mn_{0.395}Co_{0.14})_{3a}(O_2)_{6c}$ to be distinguished: both structural models correspond to an M/O ratio equal to 0.465. The reliability factors were slightly smaller in the case of the hypothesis of local oxygen vacancies ($R_B = 5.57\%$; $R_{wp} = 17.2\%$ vs $R_B = 6.0\%$; $R_{wp} = 20.2\%$), due to an additional refined parameter. Comparison between the experimental and the calculated XRD patterns is given in Figure 8b for the structural hypothesis of an oxygen loss with a contraction of the oxygen lattice (i.e., $(Li_{0.74}Ni_{0.04}\square_{0.22})_{3b}(\square_{0.11}Ni_{0.355}Mn_{0.395}Co_{0.14})_{3a}(O_2)_{6c}$). A good minimization of the difference is observed.

This XRD study combined with redox titrations has thus revealed that the irreversible "plateau" observed for $Li_{1.12}(Ni_{0.425}Mn_{0.425}Co_{0.15})_{0.88}O_2$ at 4.5 V vs Li^+/Li is associated to significant structural modifications: (i) a cation reorganization within the transition metal layers as shown by the loss of the superlattice reflections, (ii) an oxygen loss as shown by a change of the M/O ratio (0.465 for $Li_{0.73}(Ni_{0.425}Mn_{0.425}Co_{0.15})_{0.88}O_{2-\delta}$" vs 0.44 for the pristine material), and (iii) a cation migration from the slab to the interslab space.

5. Magnetic measurements. The magnetization versus field plots obtained at 5 K were compared for the reintercalated materials $Li_{0.93}(Ni_{0.425}Mn_{0.425}Co_{0.15})_{0.88}O_2$ (deintercalated up to the beginning of the "plateau" and reintercalated) and $Li_{0.73}(Ni_{0.425}Mn_{0.425}Co_{0.15})_{0.88}O_{2-\delta}$ (deintercalated up to the end of the "plateau" and reintercalated), with that of the pristine material (see Supporting Information, Figure S3). The remnant magnetization observed for $Li_{0.73}(Ni_{0.425}Mn_{0.425}Co_{0.15})_{0.88}O_{2-\delta}$" is significantly higher (∼6 emu/mol at 0 Oe and 5 K) than those observed for $Li_{0.93}(Ni_{0.425}Mn_{0.425}Co_{0.15})_{0.88}O_2$ and the pristine material (∼0 emu/mol at 0 Oe and 5 K), suggesting also the largest amount of paramagnetic ions in the interslab space for $Li_{0.73}(Ni_{0.425}Mn_{0.425}Co_{0.15})_{0.88}O_{2-\delta}$. Indeed, according to previous studies, the presence of paramagnetic ions in the interslab space leads to strong 180° antiferromagnetic M−O−M

interactions between the slab and the interslab space and thus to the formation of ferrimagnetic clusters.[44,45] The higher the amount of paramagnetic species in the interslab space, the larger the remnant magnetization. Note that about the same average transition metal oxidation state was found for $Li_{0.93}(Ni_{0.425}Mn_{0.425}Co_{0.15})_{0.88}O_2$ (oxid. state = 3.45) and $Li_{0.73}(Ni_{0.425}Mn_{0.425}Co_{0.15})_{0.88}O_{1.89}$ (oxid. state = 3.39), showing thus that there is about the same amount of paramagnetic ions in these materials. The largest remnant magnetization observed for $Li_{0.73}(Ni_{0.425}Mn_{0.425}Co_{0.15})_{0.88}O_{2-\delta}$ reveals thus the largest amount of paramagnetic ions in the interslab space. The magnetic data would therefore also confirm, in good agreement with the Rietveld refinements of the XRD data, a cation migration from the slab to the interslab space during the "plateau".

Discussion

As shown by lithium and redox titrations and as confirmed by the cell parameters variation, the average transition metal oxidation state remains almost constant during the "plateau" despite a further significant lithium deintercalation. At this stage, both an oxygen loss mechanism[9] and/or a Li^+/H^+ exchange mechanism [9,18] could be accepted in order to explain the observed "plateau". Nevertheless, ^1H NMR experiments have shown that the Li^+/H^+ exchange reaction is not associated with the "plateau" itself. A Li^+/H^+ exchange reaction was sometimes observed, but as a side reaction: indeed, especially at low rate electrolyte degradation and thus production of H^+ species at the surface of the positive electrode, materials can be promoted at high voltages. As shown especially by analysis of the XRD data and redox titration results and as will be discussed hereafter, the irreversible overcapacity phenomenon observed on the "plateau" is actually associated to an oxygen loss associated to the lithium deintercalation.

As soon as the average oxidation state of the transition metal ions gets stabilized to 3.89 (with, if it occurs, only a partial oxidation of cobalt), we propose the following mechanism to explain the further removal of lithium ions from the structure. By analogy with that suggested by other authors for Li_2MnO_3,[46] an electrochemical oxidation of the oxygen ions would occur followed immediately by an oxygen loss to stabilize the electrode surface:

$$Li_{0.60}Ni^{III}_{0.02}Ni^{IV}_{0.354}Mn^{IV}_{0.374}Co^{III}_{0.102}Co^{IV}_{0.03}O_2$$

$$\downarrow \text{ lithium deintercalation / oxygen oxidation}$$

$$Li_{0.60-\varepsilon}Ni^{III}_{0.02}Ni^{IV}_{0.354}Mn^{IV}_{0.374}\,Co^{III}_{0.102}Co^{IV}_{0.03}(O_2)^{-4+\varepsilon} + \varepsilon\, Li^+ + \varepsilon\, e^-$$

$$\downarrow \text{ oxygen loss}$$

$$Li_{0.60-\varepsilon}Ni^{III}_{0.02}Ni^{IV}_{0.354}Mn^{IV}_{0.374}\,Co^{III}_{0.102}Co^{IV}_{0.03}O_{2-\varepsilon/2} + \varepsilon/4\, O_2$$

The overall reaction can be considered as an Li_2O extraction from the material. Oxygen vacancies would be formed at the surface of the material, simultaneously with lithium deintercalation which occurs in the bulk. As the electrical neutrality must be achieved within the material, at the microscopic scale one has to consider either the formation of oxygen vacancies and diffusion of oxygen ions from the bulk to the surface or the diffusion of transition metal ions to the bulk thanks to the vacancies formed upon lithium deintercalation from the transition metal sites (3a):

(i) In the first hypothesis the cationic distribution is not modified and the oxygen vacancies are distributed in the lattice leading to the formation of MO_5 square pyramid environments. The final structure would be in that case well described by the $(Li_{0.70}Ni_{0.04}\square_{0.26})_{3b}(\square_{0.16}Ni_{0.334}Mn_{0.374}Co_{0.132})_{3a}(O_{1.89}\square_{0.11})_{6c}$ formula.

(ii) In the second model the oxygen evolution from the surface and the migration of transition metal ions to the bulk lead to a material densification. The final structure would be in that case well described by the $(Li_{0.74}Ni_{0.04}\square_{0.22})_{3b}(\square_{0.11}Ni_{0.355}Mn_{0.395}Co_{0.14})_{3a}(O_2)_{6c}$ formula.

Figure 9 gives a schematic representation of these two models. Note that the sole results given in this paper do not allow distinguishing between these two structural hypotheses even if the oxygen migration in the solid is more unlikely to occur. As reported elsewhere in detail,[37] additional results obtained by electron diffraction show that a structural reorganization occurred. As shown in Figure 10 which summarizes the electron diffraction study, the pristine material and the material recovered after one cycle before the high voltage "plateau" exhibit the superstructure, while the material that was deintercalated on the "plateau" and then reintercalated does not present any superstructure spots. This result shows that the superstructure has disappeared and thus that the transition metal cations have moved inside the lattice. This strongly supports the second mechanism, that is, an oxygen loss with a cation migration from the surface to the bulk and thus a densification of the structure.[37] Indeed, formation through oxygen loss of five oxygen environments for Ni^{4+}, Mn^{4+}, or Co^{3+}/Co^{4+} transition metal ions on the surface leads to their destabilization. Moreover, as lithium ions are deintercalated from the bulk the transition metal cations must move to the bulk for charge compensation. When it is possible, they thus migrate through face-sharing tetrahedra and get stabilized into neighboring octahedral sites previously occupied by lithium ions. This cation reorganization in the slab is therefore in agreement on the one hand, with the electron diffraction results showing a loss of the superstructure and thus of the cation ordering observed for the pristine material,[37] and on the other, with cation migration from the surface to the bulk or in other words with the lattice densification model.

These results are also in good agreement with those recently reported for $Li[Ni_{0.2}Li_{0.2}Mn_{0.6}]O_2$ by Armstrong et al.[31] They have demonstrated that oxygen loss occurs according to the second reaction mechanism we considered, that is, the lattice densification. Note that due to the large oxygen loss observed on the "plateau" for $Li[Ni_{0.2}Li_{0.2}Mn_{0.6}]O_2$ (~18% vs ~5.5% for $Li_{1.12}(Ni_{0.425}Mn_{0.425}Co_{0.15})_{0.88}O_2$), using neutron diffraction these authors were able to distinguish between the two structural models.

(44) Barra, A. L.; Chouteau, G.; Stepanov, A.; Rougier, A.; Delmas, C. *Eur. Phys. J. B* **1999**, *7*, 551.
(45) Kobayashi, H.; Sakaebe, H.; Kageyama, H.; Tatsumi, K.; Arachi, Y.; Kamiyama, T. *J. Mater. Chem.* **2003**, *13*, 590.

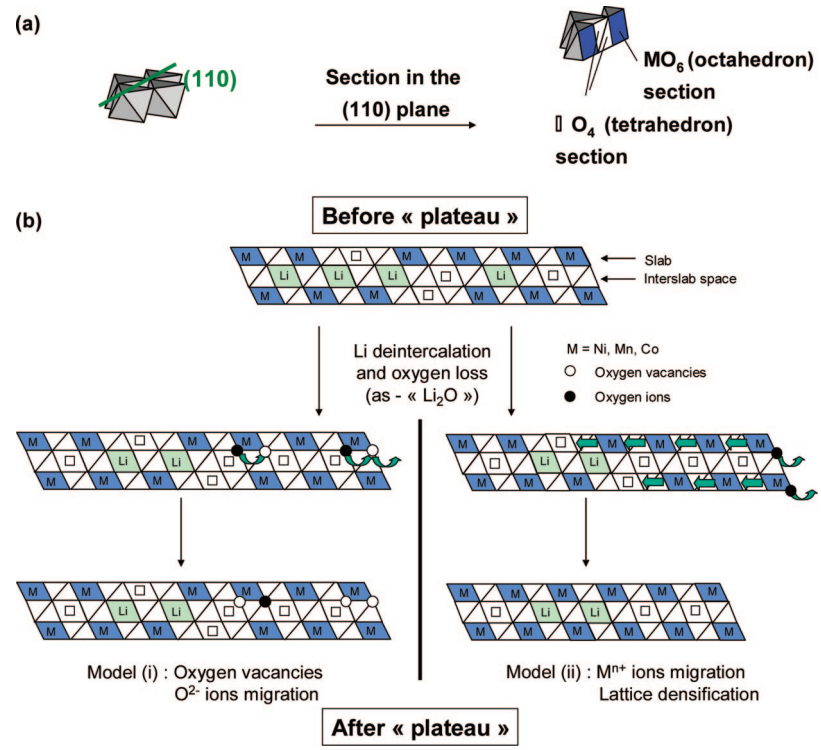

Figure 9. (a) Representation of a slab after a (110) section of an MO_2 slab; (b) schematic view in the (110) section of the $Li_y(Ni_{0.425}Mn_{0.425}Co_{0.15})_{0.88}O_2$ structure before and after the "plateau", in the case of an "oxygen migration" or "lattice densification" model. □, lithium vacancies; ○, oxygen vacancies.

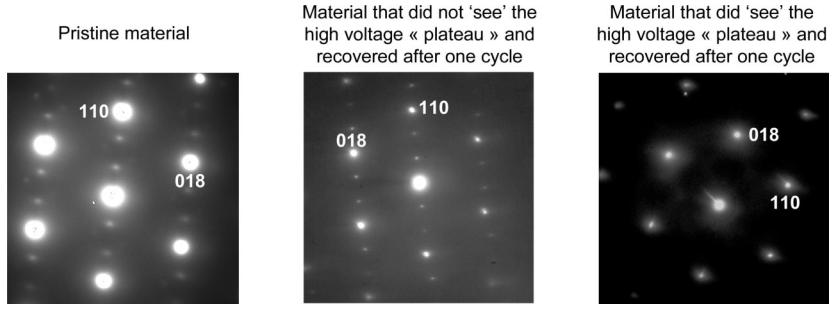

Figure 10. $[8\bar{8}1]_{hex.}$ zone axis patterns recorded for the pristine material $Li_{1.12}(Ni_{0.425}Mn_{0.425}Co_{0.15})_{0.88}O_2$, for $Li_{0.93}(Ni_{0.425}Mn_{0.425}Co_{0.15})_{0.88}O_2$ (obtained in discharge after a charge before the "plateau") and for $Li_{0.73}(Ni_{0.425}Mn_{0.425}Co_{0.15})_{0.88}O_{2-\delta}$ (obtained in discharge after a charge at the end of the "plateau"). C: graphite from the positive electrode.

Simulations have shown that, in our case, as with XRD it would not have been possible to distinguish between the two structural models (See Supporting Information, Figure S4). To conclude, in our opinion the results obtained by Armstrong et al. nicely support the mechanism we associated to the "plateau" observed at high voltage for the overlithiated $Li_{1.12}(Ni_{0.425}Mn_{0.425}Co_{0.15})_{0.88}O_2$ system. Furthermore, their results obtained for $Li[Ni_{0.2}Li_{0.2}Mn_{0.6}]O_2$ suggest that the densification mechanism we proposed is also valid in the absence of cobalt and that it can probably be generalized to overlithiated manganese-rich layered oxides.

Conclusions

The $Li_y(Ni_{0.425}Mn_{0.425}Co_{0.15})_{0.88}O_2$ ($y = 1.12, 0.78, 0.54, 0.22, 0.73, 0.93$) materials were studied to understand the mechanisms involved in the irreversible "plateau" observed upon charging a Li//$Li_{1.12}(Ni_{0.425}Mn_{0.425}Co_{0.15})_{0.88}O_2$ cell up to 5 V. Actual lithium ion extraction from the material during this "plateau" was clearly evidenced by chemical Li analysis. The redox titrations showed a continuous increase in the average oxidation state of the transition metal ions up to the beginning of the "plateau" and then no significant evolution during the "plateau", which could be explained by an oxygen loss mechanism or by a Li^+/H^+ exchange. ^1H MAS NMR data showed that no Li^+/H^+ exchange is associated to the "plateau" itself, while protons in the material are observed when parasitic side reaction of electrolyte decomposition occurs during the charge (with no link to the plateau). XRD data and redox titration results obtained for $Li_{0.73}(Ni_{0.425}Mn_{0.425}Co_{0.15})_{0.88}O_{2-\delta}$ reintercalated after a charge up to the end of the "plateau" revealed an increase of the M/O ratio, which was consistent with the oxygen loss proposed by Lu et al.[9] In a first step, two reaction mechanisms were

(46) Kim, J. S.; Johnson, C. S.; Vaughey, J. T.; Thackeray, M. M.; Hackney, S. A. *Chem. Mater.* **2004**, *16*, 1996.
(47) Berar, J.-F.; Lelann, P. *J. Appl. Crystallogr.* **1991**, *24*, 1.

proposed to accommodate the oxygen loss and to satisfy the electroneutrality rule at the microscopic scale: (i) oxygen ion migration from the bulk to the surface with the final presence throughout the material of oxygen vacancies and five oxygen environments for transition metal ions and (ii) migration of the transition metal ions from the surface to the bulk within the slabs with a global densification of the material. The disappearance of the superlattice lines in the XRD pattern and of the superstructure spots on the electron diffraction patterns indicate an irreversible cationic reorganization within the slab during the "plateau". These results support the second reaction mechanism proposed, that is, an oxygen loss at the surface with a densification of the lattice through a cation migration from the surface to the bulk. From this point of view this mechanism can be considered as the opposite of a metal oxidation (formation of NiO, for example).

Acknowledgment. The authors are grateful to F. Bonhomme (SAFT, Bordeaux, France) for fruitful discussions, to C. Denage (ICMCB) for technical assistance, and to SAFT and Région Aquitaine for financial support.

Supporting Information Available: Four figures and two table. Figure S1 gives the electrochemical curves of the Li//$Li_{1.12}(Ni_{0.425}Mn_{0.425}Co_{0.15})_{0.88}O_2$ cells used to obtain the $Li_y(Ni_{0.425}Mn_{0.425}Co_{0.15})_{0.88}O_2$ samples studied using ^{1}H MAS NMR. Figure S2 gives ^{1}H MAS NMR spectra recorded in Echo conditions at 10 kHz for $HNiO_2$, $HCoO_2$, and $Mg(OH)_2$. These spectra allowed giving the assignment of the different signals observed in the spectra recorded for $Li_y(Ni_{0.425}Mn_{0.425}Co_{0.15})_{0.88}O_2$ materials. Figure S3 gives a comparison of the magnetization vs field plots obtained at 5 K for the reintercalated materials $Li_{0.93}(Ni_{0.425}Mn_{0.425}Co_{0.15})_{0.88}O_2$ (before "plateau") and $Li_{0.73}(Ni_{0.425}Mn_{0.425}Co_{0.15})_{0.88}O_{2-\delta}$ (after "plateau"), as well as for the pristine material. An enlargement of these plots is given and reveals the largest remnant magnetization for $Li_{0.73}(Ni_{0.425}Mn_{0.425}Co_{0.15})_{0.88}O_{2-\delta}$. Figure S4 gives the neutron diffraction patterns simulated for $Li_{0.70}(Ni_{0.425}Mn_{0.425}Co_{0.15})_{0.88}O_{1.89}$ considering either the densification model or the model with oxygen vacancies. An increasing oxygen loss was shown to allow discriminating using neutron diffraction between the two structural models. Table S1 gives the structural data determined for $Li_{0.93}(Ni_{0.425}Mn_{0.425}Co_{0.15})_{0.88}O_2$ (before "plateau") and Table S2 the structural data determined for $Li_{0.73}(Ni_{0.425}Mn_{0.425}Co_{0.15})_{0.88}O_{2-\delta}$ (after "plateau") (PDF). This material is available free of charge via the Internet at http://pubs.acs.org.

CM070435M